MODELLING SOLAR MAGNETIC FLUX AND IRRADIANCE DURING AND SINCE THE MAUNDER MINIMUM

K.F. Tapping[1], D. Boteler[1,2,3], A. Crouch[1], P. Charbonneau[1], A. Manson[1], H. Paquette[2]

[1] *Herzberg Institute of Astrophysics, National Research Council, P.O. Box 248, Penticton, British Columbia, V2A 6J9, Canada. (*ken.tapping@nrc-cnrc.gc.ca*)*

[2] *Geomagnetics Laboratory, Natural Resources Canada, 2617 Anderson Road, Ottawa, Ontario, K2A 0Y3 Canada. (*david.boteler@nrcan-rnrcan.gc.ca*)*

[3] *Université of Montréal, Montréal, Québec, H3T 1J4 Canada (*ash@astro.umontreal.ca, paulchar@astro.umontreal.ca, paquette@umontreal.ca*)*

[4] *Institute for Space and Atmospheric Studies, University of Saskatchewan, Saskatoon, Saskatchewan, S7N 5E2 Canada (*alan.manson@usask.ca*)*

Received ; accepted

Abstract.

Using sunspot number as input, we construct a model for the evolution of magnetic flux from strong elements in active regions to weak remnants during the solar cycle and thence estimate the historical record of irradiance from the Maunder Minimum to the present. The magnetic flux model is a fragmentation cascade starting with strong-field elements, which fragment into weak-field elements and then into a background field. The model indicates the mean total irradiance during the Maunder Minimum was between 1 and 1.5 Wm^{-2} lower than it is at present.

Keywords: Maunder Minimum, solar variability, irradiance

1. Introduction

The history of solar irradiance variation is a critical component in understanding the solar-terrestrial climate connection and the relative role of the Sun in current climate change. However, direct measurements of solar irradiance currently cover only about three decades. Beyond that interval irradiance has to be estimated using available observations and activity indices. This entails three major difficulties: (a) the physical connection between the observed activity phenomena, such as sunspot number with irradiance is complex and difficult to quantify. Often the result is the need to use connections that are often largely empirical, (b) proxies might have to be used. In a sense this has some commonality with (a), except that here the physical connection is even less understood, but a historical high correlation between the proxy and the desired quantity justifies its use, (c) having constructed a model which necessarily incorporates elements of (a) and (b), it has to be extrapolated substantially outside the parameter space that was used to set up that model.

That there is a connection between solar variability and terrestrial environmental change is well-documented, and evident in both recent, mediaeval and geological records (see for example, Anderson, 1991). Over the last 2000 years there have been instances where solar activity fell to a low level for some decades. These have become known as the Wolf (1280-1350AD), Spörer (1420-1540AD), Maunder (1645-1715) and Dalton (1795-1825) minima. Connections between these minima and periods of anomalous global cooling were first pointed out by Eddy (1976 *a*, *b*, 1977, 1979, 1980).

The period between 1700 and the present is important in that there is a continuous record of sunspot number, which is a directly measured index of solar activity, of known pedigree with established relationships with other activity indices, and which antedates the rapid increase in anthropogenic greenhouse gases that began with the industrial revolution. A difficulty is that any models have to be driven by sunspot number or some quantity measured on Earth.

There are currently two main schools of thought in the study of solar irradiance variability. One proposes that the observed irradiance variations come from the changing relative distributions over the photosphere of different activity phenomena with different emissivities, such as sunspots, faculae and elements of the active network. It is certainly well established that the shorter-term irradiance variations follow changes in solar magnetic activity (Willson and Hudson, 1991; Fröhlich, 1994; Kuhn, 1996). It has been shown that these changes in solar irradiance correlate with bright faculae and magnetic network (Foukal and Lean, 1988). Upon this basis, using recent measurements and older proxies, Lean (2000) has estimated irradiance variations back to the Maunder Minimum. The other school proposes that to adequately model irradiance variations, some additional phenomena associated with magnetic activity need to be included. Suggestions include variations in the solar radius (Delache *et al.*, 1986; Ulrich and Bertello, 1995; Antia, 2003), large convective cells (Ribes *et al.*, 1985; Fox and Sofia, 1994; Sofia, 2004; Sofia and Li, 2004).

Considerations of irradiance variability require as clear as possible a picture of the process of solar activity. The main element of this activity is the processing and distribution of magnetic flux below, at and above the photosphere. A discussion of the magnetic interpretation of solar activity is given by Parker (1994). In the context of the photosphere and chromosphere, activity takes place primarily in *complexes of activity*, that may contain several active regions at various stages in their evolution, together with their decay products. These complexes persist for up to a dozen solar rotations. A detailed study of these complexes and their evolution is given by Gaizauskas *et al.* (1983).

Modelling irradiance is difficult. Firstly we do not fully understand the processes driving irradiance variations; the underlying physics is complex

and multifaceted, and includes phenomena below and at the photosphere. Most of the relationships we have to work with are empirical, although the correlation coefficients between total irradiance and indices such as the 10.7 cm solar radio flux are high. For example, since total irradiance is highly correlated with sunspot number, it seems logical to plot irradiance against sunspot number and extrapolate back to zero sunspot number, and then conclude that the corresponding value of irradiance is the value that would be reached if solar activity remained low for an extended period. This is almost certainly not the case. Sunspots do not cause increases irradiance; it is the accompanying active region structures, such as faculae and elements of the active network that do this. Although there might not be any sunspots, there are signs of activity during every observed minimum of the solar activity cycle; there are ephemeral regions (short-lived magnetic bipoles) forming and dissipating, and large areas of weaker magnetic flux remaining from the decay of old active regions (see the discussion in Zwaan and Harvey, 1994). Sunspots might be a good indicator of magnetic activity when present, but they are not useful when activity is low. When examining solar activity during a sustained change in the solar activity cycle, or even a temporary cessation, one needs to examine two issues: firstly, does the nature of the process by which magnetic flux is processed change, and secondly, what is the solar activity machine below the photosphere doing. There have been previous attempts at modelling the history of solar magnetic activity. The use of solar magnetic fields as a basis for irradiance modelling was examined by Harvey (1994), and more recently by Fox (2004). In work conducted since, particularly noteworthy are models by Solanki *et al.* (2000, 2002), which model the processing of magnetic flux over the solar cycle. In the case of this investigation, the input to the model has to be sunspot number, which is the only direct index of solar activity available. In this paper we develop a model for the processing of solar magnetic flux and use it to model the historical record of total irradiance.

2. The Data

2.1. Sunspot Number: N

Sunspot number is the oldest directly-measured index of solar activity, and now forms a consistent, continuous record covering more than 300 years. The main database of sunspot numbers is maintained by the Solar Influences Data Centre (SIDC) in Belgium, but available through a number of sources worldwide. The sunspot number data used in this paper, covering the period 1700 to the present, were obtained from the National Geophysical Data Center, Boulder, Colorado.The sunspot number index (more correctly referred

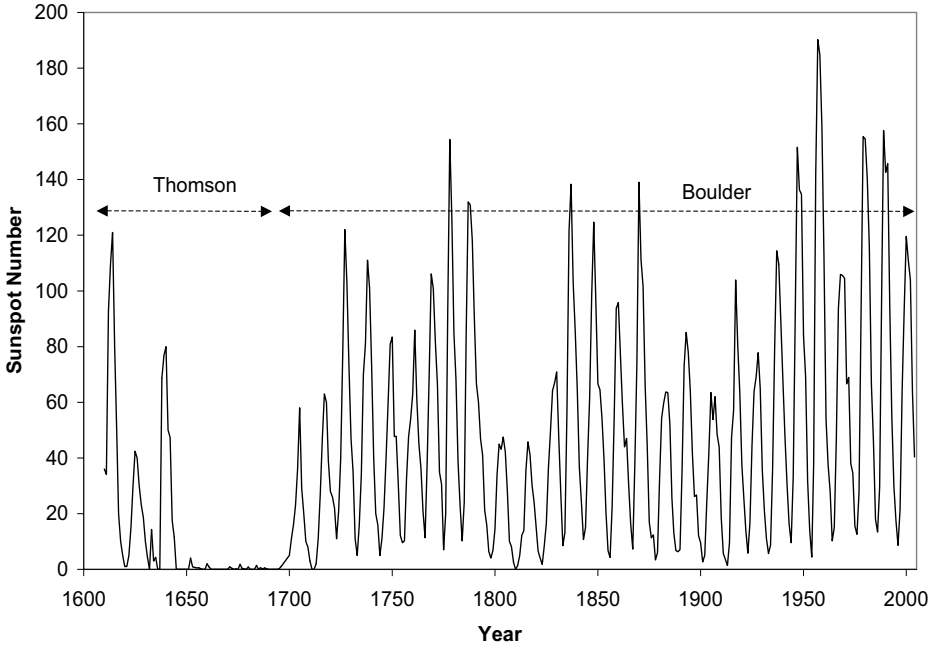

Figure 1. Sunspot number from 1610 to 2004. The data before 1700 was obtained by Thomson, through compilation of data from several sources; the data since was the standard dataset provided by the US National Geophysical Data Center.

to as the Zürich Sunspot Number) has proved itself to be a very useful indicator of the level of solar activity. Its disadvantage is that it is empirical and cannot be theoretically related to solar and active region parameters, and the slope of plots of sunspot number against other indices changes at the low-activity end, making extrapolation uncertain. However, for reasons explained later, operating the model requires sunspot data antedating the Maunder Minimum. Thomson (private communication), using research by Hoyt *et. al.* (1995*a* and *b*, 1996 and 1998*a* and *b*) made estimates of sunspot number from 1610 onwards. These have been smoothed using a running mean and attached to the other sunspot data. The resulting integrated data set is shown in Figure 1.

2.2. 10.7 cm Solar Radio Flux: $F_{10.7}$

The 10.7 cm solar radio flux values are measurements of the intensity, at 10.7 cm wavelength, of the slowly-varying component (S-component) of solar radio emission. The S-component can be observed at wavelengths from about 50 to 1 cm, but is brightest at wavelengths close to 10 cm, hence the value of measurements at 10.7 cm wavelength. It is thermal in origin, and comes from coronal plasma trapped in the magnetic fields overlying active regions. The observed brightness temperature of a slab of this trapped plasma is related to the thickness of the plasma slab and its density, and can be estimated using models of the form:

$$T_b = T_{corona}\,(1 - \exp(-\gamma z)) \tag{1}$$

where γ is the absorption coefficient and z the thickness of the plasma slab.

In active regions where the ambient magnetic fields supporting the plasma are low enough for the electron gyrofrequency (roughly $f_B = 2.8 \times 10^6 B$ Hz, where B is in Gauss) is less than about a third of the observing frequency, the main contributor to γ is free-free interactions between thermal electrons and ions. In places where the magnetic fields are stronger, for example over sunspots, thermal gyroresonance can produce much brighter emission by dramatically increasing γ. A more detailed discussion of the S-component and its origins are given in monographs by Kundu (1965) and Krüger (1979), and in Tapping and Harvey (1994). The intensity of the S-component at 10.7 cm wavelength, which is known as the 10.7 cm solar radio flux, or $F_{10.7}$, is a well-established index of solar activity. A specific discussion of the 10.7 cm solar radio flux is given in Tapping (1987). The S-component is a composite of contributions from all the active regions on the solar disc plus emissions originating outside active regions. Studies of active region radio sources as contributors to the S-component have been made by Tapping and Zwaan (2002) and Tapping *et al.* (2003). Annually-averaged data since the beginning of the programme in 1947 are shown in Figure 2. The 10.7 cm solar radio flux is given in solar flux units (1 solar flux unit (sfu) $\equiv 10^{-22}\mathrm{Wm}^{-2}\mathrm{Hz}^{-1}$).

2.3. Magnetic Flux

For more than two decades, the magnetograph at the National Solar Observatory at Kitt Peak has been used to measure the distribution of magnetic flux at the photosphere with near-arc-second resolution. The instrument is essentially a high-angular resolution spectrometer that can be used to measure the Zeeman splitting of selected photospheric spectral lines). Harvey (1992) analyzed magnetograms over more than a solar activity cycle

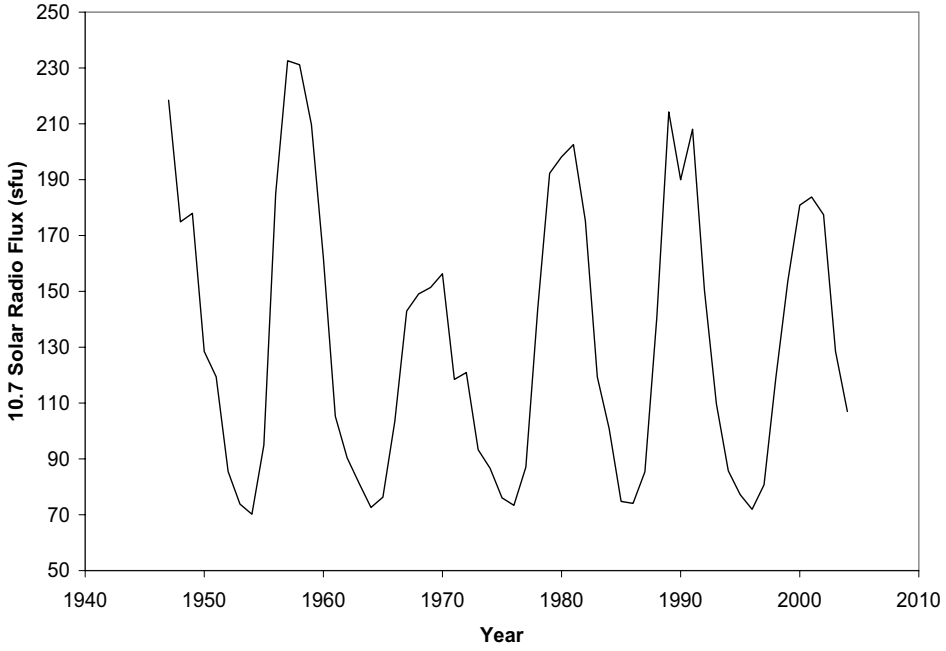

Figure 2. Annually-averaged values of the 10.7 cm solar radio flux from 1947 to present.

to estimate the contributions to the total magnetic flux coming from the various types of magnetic structure, including sunspots, faculae, the active network, the intra-network fields and possibly a background component. She found that to a very large degree, the magnetic elements measured by the magnetograph fall into two distinct classes (see also Zwaan and Harvey, 1994): *strong-field elements* having average magnetic field strengths higher than a certain threshold value, and other elements, located outside active regions, with average magnetic field strengths smaller than this value. Moreover, she demonstrated that this threshold magnetic field strength could be varied over the range 25-40 Gauss without significantly affecting the relative budget, so clearly different populations are identified. Elements having intermediate values for magnetic field strength exist only transiently during region fragmentation. For reasons discussed later in the paper, we divide the weaker-field elements into two magnetic flux contributions: *weak-field*

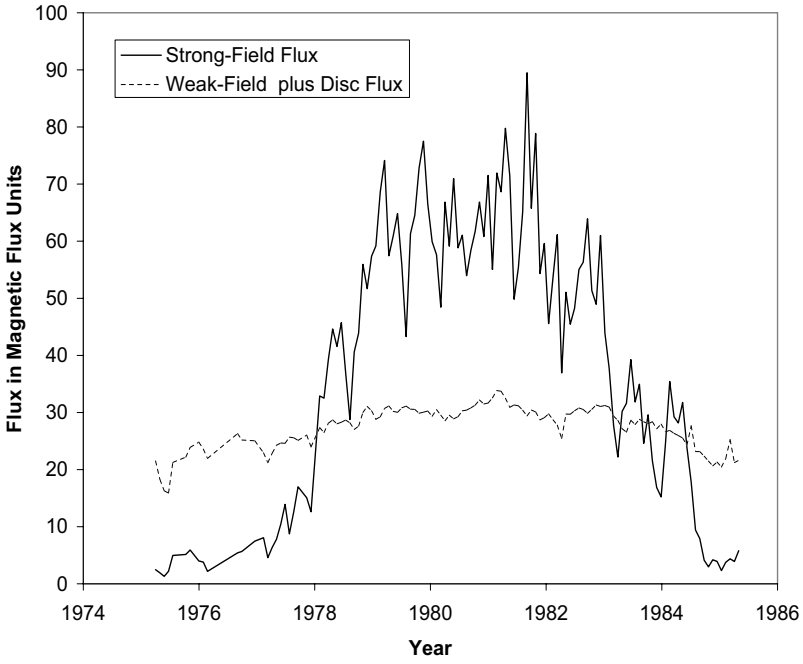

Figure 3. Rotationally-averaged total disc magnetic flux in strong-field and other (weak + disc) magnetic flux elements over a solar activity cycle.

elements and *disc elements*. Figure 3 shows a plot of the total magnetic flux in strong-field elements and that in weak-field plus disc elements over a solar activity cycle. Following the practice used by Harvey, all the magnetic flux values used here, unless it is stated otherwise, are given in *magnetic flux units* (1 magnetic flux unit (mfu) $\equiv 10^{22}$ Maxwells).

The strong-field elements lie in active regions and in elements of the active network. Their intrinsic field strengths range from about 1,000 Gauss (in network elements) to 3,000 Gauss (in sunspots). Since these elements often lie below the resolution of the magnetograms, the field strengths measured are averages over the element and consequently smaller. Ephemeral regions are considered to be simply the small-scale end of the size distribution of active regions. Setting them aside as a separate category of active structures is an artifact of previous lines of research (Zwaan and Harvey, 1994). The

weak-field elements include the *intra-network field* (INF), which are probably a product of collapse of field lines in network elements, that due to their weakness, are trapped between the canopy of strong field lines connecting the network elements, and which repeatedly emerge and submerge above and below the photosphere between their end-points. The INF occurs all over the photosphere. In Figure 3, the total magnetic flux in weak-field elements shows two components: one that varies over the solar activity cycle, in phase with the total magnetic flux in strong-field elements, and one that forms a more or less constant background of about 20 mfu. We assume three magnetic flux contributions: the strong-field magnetic flux Φ_S, the weak-field magnetic flux Φ_W, and the background disc magnetic flux, $\Phi_\odot$ (about 20 mfu in the figure). The relationships between these contributions is discussed in a later section.

2.4. Irradiance

Through a succession of instruments, irradiance measurements have been made over almost three solar activity cycles so far, from 1978 to the present. The instruments and observation record intervals are presented in Table I.

Table I. Summary of the instruments used to observe the total solar irradiance.

Radiometer	Satellite	Extent of Data Record
H-F	Nimbus 7	1978 - 1992
ACRIM I	SMM	1980 - 1989
ERBE	ERBS	1984 - Present
ACRIM II	UARS	1991 - 2001
VIRGO	SOHO	1996 - present
ACRIM III	ACRIM-Sat	2000 - present

A review of the measurements, measurement methods and instrumentation is given by Fröhlich *et al.* (1991). Integration of these separate data sets into a single, consistent and calibrated record required a considerable effort, but has been achieved very successfully. These data sets and the integration task are described by Pap and Fröhlich (1999) and Fröhlich (2004), and references therein (see also Fröhlich and Lean 1998*a* and b). This integrated irradiance database was obtained from PMOD/WRC, Davos, Switzerland. The integration of six data sets of irradiance measurements made using different instruments into a single irradiance record is a major achievement. The irradiance values used in this paper are annual averages. These values

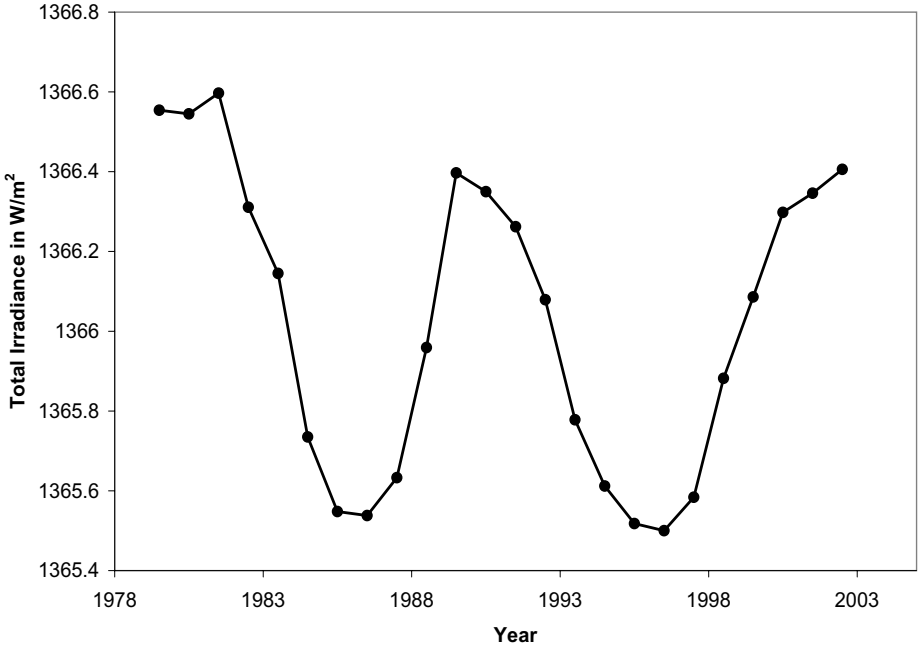

Figure 4. Annually-averaged values of measured total irradiance over almost three solar activity cycles.

are plotted in Figure 4. The modulation of the total irradiance by the solar activity cycle is clearly visible.

3. The Irradiance Model

There are two main lines of argument in modelling irradiance variability. On one hand, some researchers, for example Lean *et al.* (1998), Solanki and Unruh (1998) and Spruit (2000), along with other references listed earlier in this paper, suggest that the observed variations in irradiance over the solar cycle can be accounted for purely in the changes in sunspot and facular areas, This would make irradiance variability a purely photospheric phenomenon. On the other hand, other workers, such as Gray and Livingston (1997),

Sofia and Li (2004) suggest small changes in global photospheric temperature are involved. These would have to be the result of sub-photospheric processes. That the solar interior might be more deeply involved is suggested through helioseismological studies and magnetic modelling (Woodard, 1987; Bhatnagar *et al.*, 1999; Kuhn, 2004).

When averaging data over a year, the properties of active regions and other classes of magnetic structure become sufficiently consistent that we can write the following very general model for total irradiance just beyond the Earth's atmosphere:

$$I = I_\infty \Psi(t) \xi(t) D(t) \tag{2}$$

I_∞ is the long-term average irradiance, which is proportional to the rate at which energy is produced in the Sun's core, which can be assumed constant over the timescales considered here, $\Psi(t)$ describes the modulation of energy flow between the core and the photosphere, $\xi(t)$ modulation of the rate at which the photosphere radiates energy into space, and $D(t)$ the changing distance between the Earth and Sun. Since in this study we use annually-averaged data, $D(t) = 1$. The internal thermal time-constant is high and the heat capacity large, so modulation of irradiance has no effect on core conditions, provided that:

$$1 = \frac{1}{T} \int_1^T \Psi(t) \xi(t) dt \tag{3}$$

where T is a duration (10^6 years?) larger than the internal thermal time constant but small compared with solar evolutionary timescales . That is, when averaged over a suitably long internal thermal time-scale, the rate of radiation of energy to space has to be equal to the rate at which it is produced in the Sun's core.

The possibility that irradiance variations may entirely or in part be due to modulation of the energy flow between core and surface has been investigated by various workers (For example, see Sofia and Li, 2004). The presence of sub-photospheric magnetic flux, at least in part as a component of solar activity, contributes to the sub-photospheric pressure and to the energy transfer efficiency. Since the modulation of the irradiance is small, we use the approximation:

$$\Psi(t) = 1 + \beta \Phi_T \tag{4}$$

where β is a constant ($<< 1$), having the units mfu^{-1}. and Φ_T the total amount of photospheric magnetic flux.

If the total irradiance comprises contributions from all the active structures on the disc plus a background contribution from the rest of the solar disc, the function $I_\infty \xi(t)$ is given by:

$$I_\infty \xi(t) = \sum_i \epsilon_i A_i + \left(A_\odot - \sum_i A_i \right) \epsilon_0 = \sum_i (\epsilon_i - \epsilon_0) A_i + A_\odot \epsilon_0 \qquad (5)$$

where A_i is the total area covered by the ith class of photospheric structure and ϵ_i the emissivity of that class. The total photospheric area is $A_\odot$. If the total magnetic flux and average magnetic field strength in the ıth structure class are respectively Φ_i and $\bar{B}_i$, $I_\infty \xi(t)$ becomes:

$$I_\infty \xi(t) = \sum_i (\epsilon_i - \epsilon_0) \frac{\Phi_i}{\bar{B}_i} + A_\odot \epsilon_0 = \sum_i \eta_i \Phi_i + I_\odot \qquad (6)$$

where, combining the constants, $\eta_i = (\epsilon_i - \epsilon_0)/\bar{B}_i$ and $A_\odot \epsilon_0 = I_\odot$. The quantity $I_\odot$ is an irradiance that would not be reached in practice, because it would require a photosphere completely devoid of magnetic flux.

Therefore the total irradiance model is:

$$I = (1 + \beta \Phi_T) \left(\sum_i \eta_i \Phi_i + I_\odot \right) \qquad (7)$$

To evaluate this equation we need to identify the various magnetic component classes and estimate the total magnetic fluxes they contain.

4. Modelling Historical Magnetic Flux Contributions

The plot in Figure **??** shows the strong-field magnetic flux varies strongly over the solar activity cycle, falling close to zero at the solar activity minimum. The rest of the magnetic flux (Φ_* say) shows two characteristics, a small variation in phase with the strong-field magnetic flux, and background of about 20 mfu. We propose that Φ_* comprises (at least) two distinct components. If we assume that Φ_* receives flux from Φ_S and loses flux primarily through an exponential process, Φ_* will have two distinct properties both related to the rate of flux dissipation: there will be a minimum (base) level related to the rate of flux dissipation, and there will be a phase delay between the variations of Φ_S and Φ_*. If Φ_S can, for this restricted purpose, be represented by the equation $A_S(1 + \sin(\Omega t))$ where Ω is the angular frequency of the solar cycle, and the dissipation by $\exp(-t/\tau_*)$, then:

$$\Phi_* = A_* \left(\tau_* + \frac{1}{\tau_*^{-2} + \Omega^2} \left(\frac{1}{\tau_*} \cos(\Omega t) + \Omega \sin(\Omega t) \right) \right) \qquad (8)$$

where A_* is a constant having the the dimensions of magnetic flux. The maxima and minima are given by $\Phi_*(\text{extrema}) = A_* \left(\tau_* \pm (\Omega^2 + \tau_*^{-2}) \right)$. The phase difference between Φ_S and Φ_* is $\Delta\phi = \tan^{-1}(\Omega \tau_*)$.

In the plots, the phase difference between the variations in Φ_S and Φ_* is small; there is no sign of a loop in a plot of Φ_* against Φ_S (shown in Figure 7, later in this paper), which suggests the time delay between the variations in the two quantities is no more than a year or two.

Define a modulation index as below:

$$m = \frac{\Phi_*(\max) - \Phi_*(\min)}{\Phi_*(\max) + \Phi_*(\min)} = \tau_*^{-1}(\Omega^2 + \tau_*^{-2})^{-1/2} \tag{9}$$

For Φ_* we obtain $m \approx 0.2$. If the angular frequency of the solar activity cycle is about 0.6 radians/year, the above equation yields $\tau_* \approx 8$ years, which would give rise to a phase shift far larger than is observed. Therefore, on the basis of exponential decay, the base level of the magnetic flux is a separate component of magnetic flux. We therefore divide Φ_* into two components: the weak-field flux and the disc flux, represented as Φ_W and $\Phi_\odot$ respectively. In particular the strong-field flux comprises contributions from several or more different classes of magnetic structure, the main ones being sunspots and faculae. However, if when averaged over all regions over whole years, their relative contributions to the total flux remain the same, we can treat the strong-field flux as a single parameter of homogenous properties. We make similar assumptions for the weak and disc fluxes.

We assume that almost all new magnetic flux emerges as strong-field elements in active regions. When these regions decay, about 70% of the magnetic flux submerges again close to where it emerged. The rest disperses away across the photosphere as weak-field elements. Most of it diffuses poleward and becomes part of the polar field. Most of the weak-field submerges or otherwise dissipates and a small amount becomes part of the disc flux. Part or most of the disc flux probably originates in other ways. However, we assume that the other contributions to the disc flux vary over timescales long compared with those applicable here. We estimate the strong-field magnetic flux Φ_S, and then model the other components directly or indirectly from it.

In the modelling process we use the historical sunspot record to estimate the 10.7 cm solar radio flux, from which we derive the strong-field magnetic flux. Then, using the formulae above, we estimate the weak-field and disc fluxes.

4.1. From Sunspot Number to Strong-Field Magnetic Flux

4.1.1. *N to* $F_{10.7}$

Figure 5 shows a plot of the 50+ years of annually averaged 10.7 cm solar radio flux data ($F_{10.7}$) plotted against sunspot number (N). The relationship between them is clear enough for a good, albeit empirical model to be established. The change in slope at the low-activity end of the plot stands

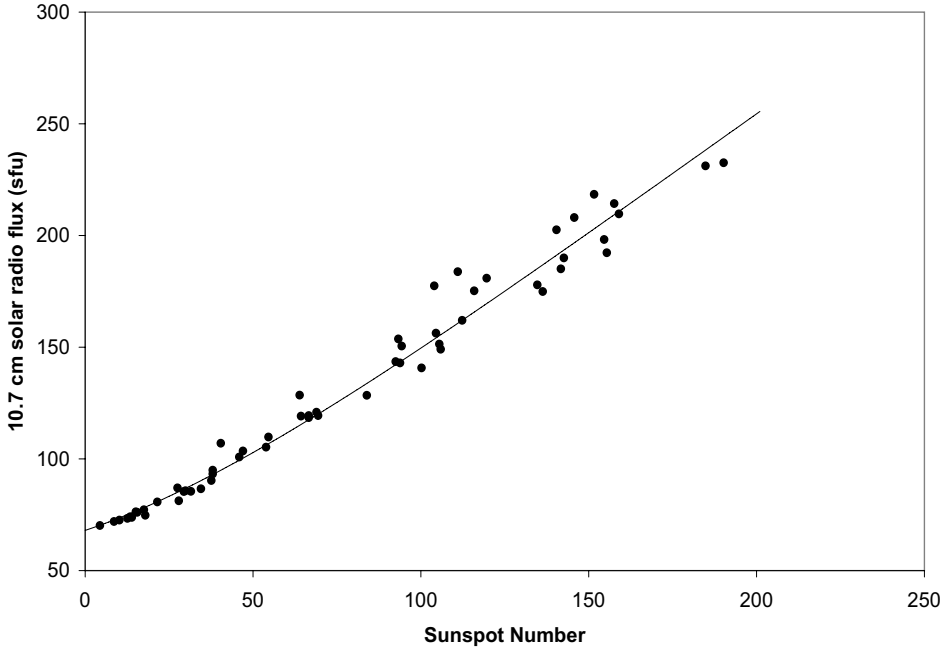

Figure 5. Annually-averaged values of the 10.7 cm solar radio flux plotted against similarly-averaged sunspot number data. The fitted equation discussed in the text is also shown.

out clearly enough for it to be described adequately by a fitted empirical function, which is also shown in the plot:

$$F_{10.7} = \frac{1}{2} N \left(2 - \exp(-0.01N)\right) + 68 \ , \qquad [sfu] \tag{10}$$

4.1.2. *$F_{10.7}$ to Φ_S*

Since the 10.7 cm solar radio flux originates primarily over active regions, and the total amount of trapped plasma producing the emission is related to the amount of magnetic flux in active regions, a correlation between $F_{10.7}$ and Φ_S, the total amount of magnetic flux in strong-field elements (which lie primarily in active structures) would be expected, and is observed. Figure 6 shows a plot of the total amount of magnetic flux in strong-field elements

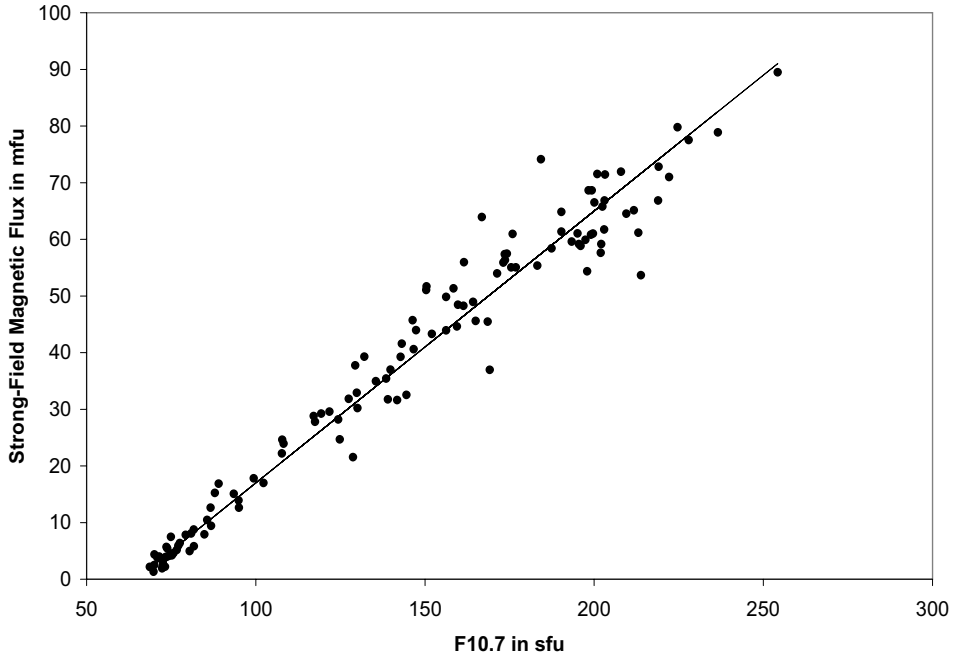

Figure 6. Rotationally-averaged values of the strong-field magnetic flux plotted against similarly-averaged values of the 10.7 cm solar radio flux, over the period 1975-1985.

plotted against the 10.7 cm solar radio flux. The data are rotational averages, over the period 1975-85, about one solar activity cycle. The correlation is strong ($R^2 = 0.96$) and linear. The fitted relationship is:

$$\Phi_S = a_S F_{10.7} + b_S \tag{11}$$

where $a_S = 0.468$ and $b_S = -28.995$. The strong-field magnetic flux obtained in this way is used as the input to the magnetic flux processing model.

4.2. Strong-Field Magnetic Flux to Weak-Field Magnetic Flux

Figure 7 shows rotationally and annually-averaged values of the weak-field + background magnetic flux plotted against the strong-field magnetic flux for one complete solar rotation, together with the results obtained using the model discussed in this section. Four characteristics stand out: (a) there is a correlation between the two quantities, (b) the relationship is not a linear one, and (c) when $\Phi_S = 0$, there is a background value of about 20 mfu. Finally, (d) if there were a significant time delay between changes in Φ_S and $\Phi_W + \Phi_\odot$, over a solar cycle the plot would form an ellipse. These is no sign of one, suggesting that the two quantities vary in phase with a time delay not exceeding one solar rotation.

Modelling flux transfer on a region by region basis would be a futile exercise. However, averaging over all sources over entire years makes it possible. Active regions are fairly stable structures, and when they start to decay, magnetic flux is lost as fragments breaking away around the perimeter of the region. We therefore assume that the rate of loss of (strong-field) magnetic flux from a region, on the average over many regions, can be assumed to be proportional to the perimeter of the region, which in turn is approximately the square root of the area A, where $A = \Phi_S/\bar{B}_S$ and $\bar{B}_S$ is the average magnetic field strength in strong-field elements. Therefore, if the loss process is exponential, the rate of change of the weak-field magnetic flux is:

$$\frac{\partial \Phi_W}{\partial t} = a_W {\Phi_S}^{1/2} - \frac{1}{\tau_W}\Phi_W \tag{12}$$

The time-constant τ_W is the characteristic time with which the weak-field flux dissipates. If there is no detectable phase delay between Φ_S and Φ_W when averaged over whole solar rotations, which, as indicated at the beginning of this section, τ_W cannot be more than a year or two. Since this is the averaging timescale for the irradiance calculation, the time-derivative is small, so:

$$\Phi_W = a_W \tau_W \Phi_S^{1/2} \tag{13}$$

This is superimposed upon a background of $\Phi_\odot$, which could be a constant or a variable with time.

4.3. Weak-Field Magnetic Flux to Disc Magnetic Flux

We assume that the weak-field magnetic flux is in turn removed by a mixture of submergence and transfer of magnetic flux to the disc magnetic flux $\Phi_\odot$. If the disc magnetic flux varies slowly, as we would expect, and the weak-field magnetic flux varies with a delay with respect to the strong-field magnetic

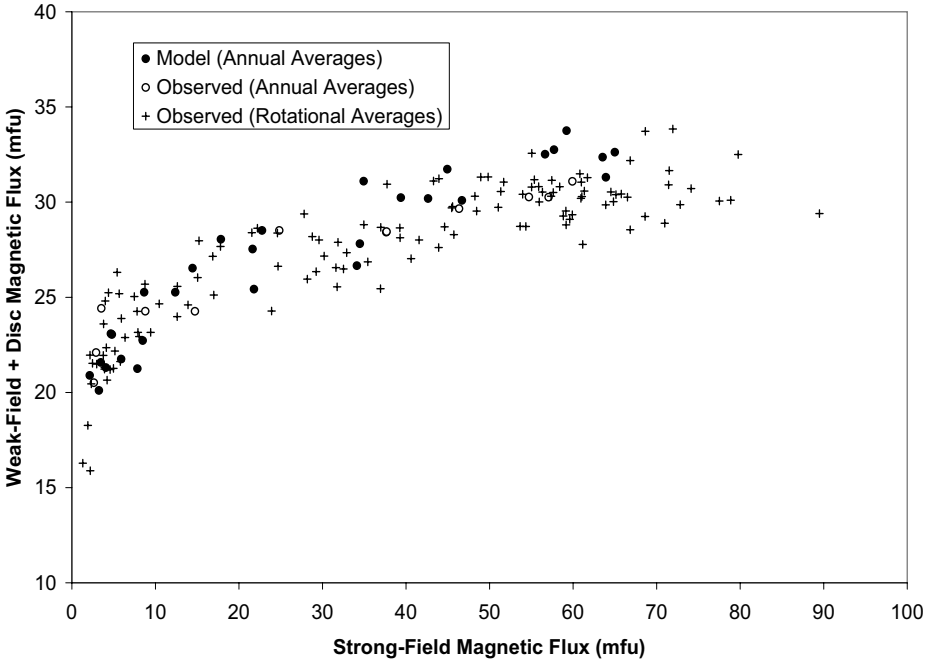

Figure 7. Rotationally averaged and annually-averaged weak-field plus disc magnetic flux plotted against similarly-averaged values of the strong-field magnetic flux, plus the model discussed later in this paper.

flux that is less than one solar rotation, the bulk of the flux must be lost by submergence, with a smaller fraction falling further down the cascade into the disc magnetic flux. The disc magnetic flux $\Phi_\odot$ is assumed to be lost entirely by submergence or other dissipation. The rate of change of the disc magnetic flux is given by:

$$\frac{\partial \Phi_\odot}{\partial t} = a_0 \Phi_W - \frac{1}{\tau_0} \Phi_\odot \tag{14}$$

Over suitably small time increments:

$$\Phi_\odot \Rightarrow \Phi_\odot + \frac{\partial \Phi_\odot}{\partial t} \Delta t \tag{15}$$

If the variation is slower than the 1-year resolution of the model, and $\Delta t = 1$:

$$\Phi_\odot \Rightarrow \Phi_\odot + a_0 \Phi_W - \frac{1}{\tau_0}\Phi_\odot \tag{16}$$

Once again the only way to estimate the coefficients is by fitting. Only one cycle is available where the measured total magnetic flux has been broken into its components. This is not really enough data for useful fitting. Fortunately, from 1977 to the present, the National Solar Observatory at Kitt Peak has provided measurements of B_{av}, the average magnetic field strength over the sphere. Ideally, this would be related to the total magnetic flux over the solar sphere by the obvious relationship: $\Phi_T = 4\pi R_\odot^2 B_{av} = 6.16 B_{av}$, where Φ_T is in mfu and B_{av} is in Gauss. However, factors like magnetic geometry, and the effects of foreshortening as the solar limb is approached, are likely to change the constant 6.16 to some other value. Plotting Φ_T against B_{av} gives a constant of 4.6 ($R^2 = 0.91$). So we assume $\Phi_T = 4.6 B_{av}$.

This equation uses B_{av} to produce estimates of Φ_T that are consistent with the measurements of the different magnetic flux components. Using the methods described in previous sections we estimate Φ_S and Φ_W. Obtaining the disc magnetic flux $\Phi_\odot$ requires values for an amplitude a_0 and a time delay τ_0. We estimate the "observed" $\Phi_\odot$ by subtracting the modelled Φ_S and Φ_W from observed values of Φ_T and those estimated using B_{av}, and then adjust a_0 and τ_0 for the best fit. We obtain $a_0 = 0.29$ and $\tau_0 = 12.7$ years, which is roughly the duration of the solar activity cycle. It is rather surprising though that this suggests roughly 30% of the weak-field magnetic flux goes into the background (disc) magnetic flux. This fraction is maybe rather large. The observed and modelled disc magnetic fluxes are shown in Figure 8, along with the total magnetic flux, so that the phase difference between the variations of the disc magnetic flux and the solar activity cycle can be distinctly seen.

4.4. Estimating Φ_S, Φ_W and $\Phi_\odot$ since 1700

Since the model includes elements estimated from previous values, modelling the magnetic field flux components during the Maunder Minimum requires the start of the modelling calculation at a date a few solar activity cycles prior to the advent of the Minimum. Sunspot data prior to the Maunder Minimum are very patchy. Fortunately Thomson (private communication) has provided estimated sunspot data before and into the Maunder Minimum. The estimated record of the strong, weak and disc magnetic flux components during and since the Maunder Minimum are shown in Figure 9.

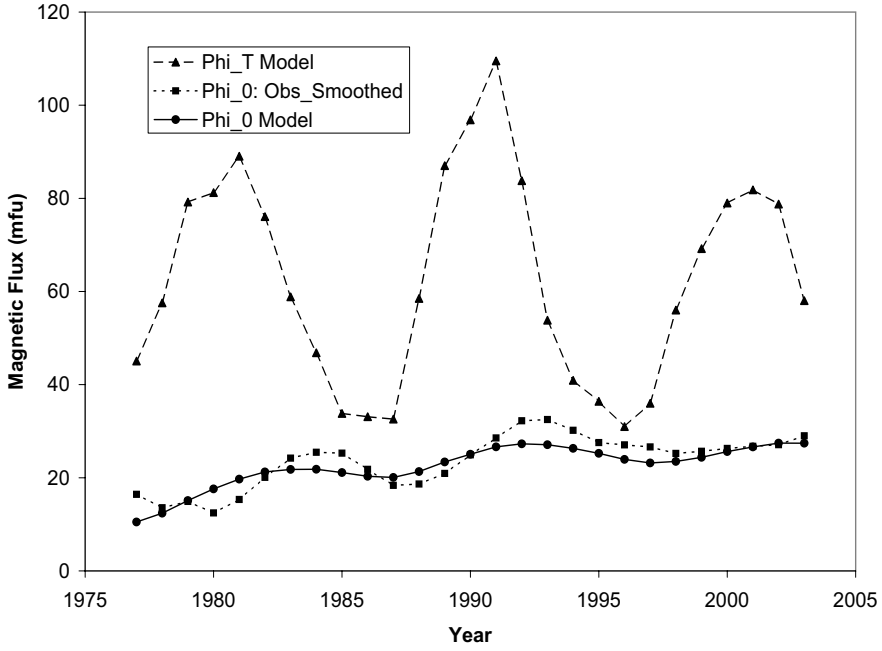

Figure 8. Observed and modelled disc magnetic flux, together with the total modelled magnetic flux, which is included for comparison to show the solar activity cycle. The disc magnetic flux varies almost in quadrature with the total magnetic flux.

5. Modelling Historical Irradiance

In terms of the identified magnetic flux components, the model for composite irradiance (equation 7) becomes:

$$I = (1 + \beta\Phi_T)\,(\eta_S\Phi_S + \eta_W\Phi_W + \eta_0\Phi_\odot + I_\odot) \tag{17}$$

where the $1 + \beta\Phi_T$ approximates the modulation of radial energy flow due to the sub-photospheric magnetic flux.

Sunspot blocking is an important consideration of solar irradiance variability. Assuming the relative fraction of sunspot magnetic flux in the strong-field flux does not change very much, the constants can be absorbed into the overall constants of proportionality, and we can consider the strong-field

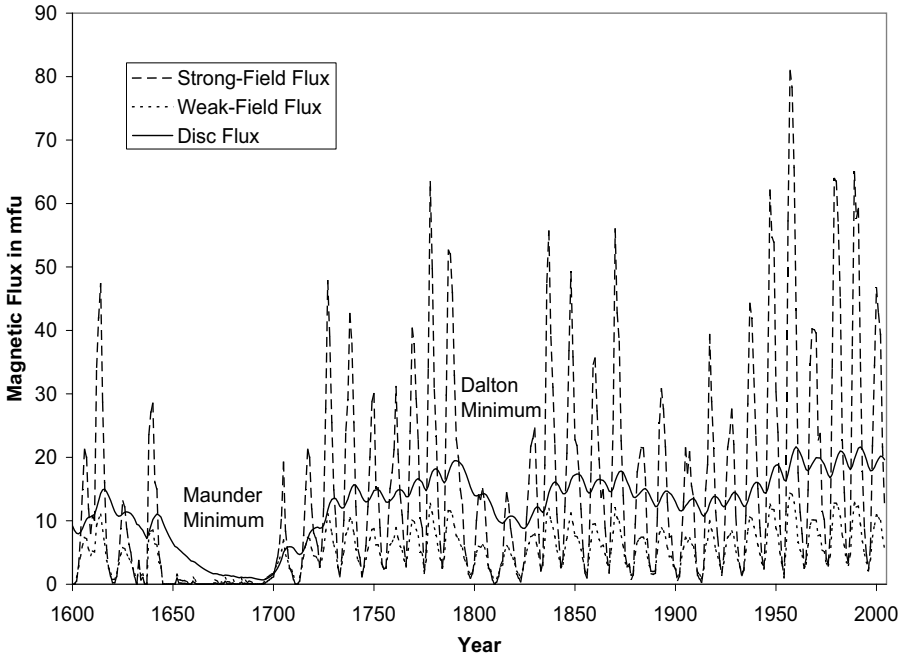

Figure 9. Modelled strong-field, weak-field and disc magnetic flux from before the Maunder Minimum to the present. The Dalton Minimum is also identified.

magnetic flux contribution to irradiance as a single contribution, with no need to subdivide it.

To estimate the values of η for the various magnetic flux components we take the annually-averaged irradiance measurements, together with the modelled Φ values and find the values giving the best fit. In all cases we found β to be very small, $< 10^{-5}$ mfu^{-1}, with only an insignificant effect upon the irradiance, so sub-photospheric modulation, formulated in the manner here, is not a factor, and we simplify the model to:

$$I = \eta_S \Phi_S + \eta_W \Phi_W + \eta_0 \Phi_\odot + I_\odot \tag{18}$$

This reduces the number of parameters to be fitted. By optimizing the fit of the modelled to the observed irradiance values, we obtain: $\eta_S = 0.006$, $\eta_W = 0.06$, $\eta_0 = 0.024$ and $I_\odot = 1364.7$.

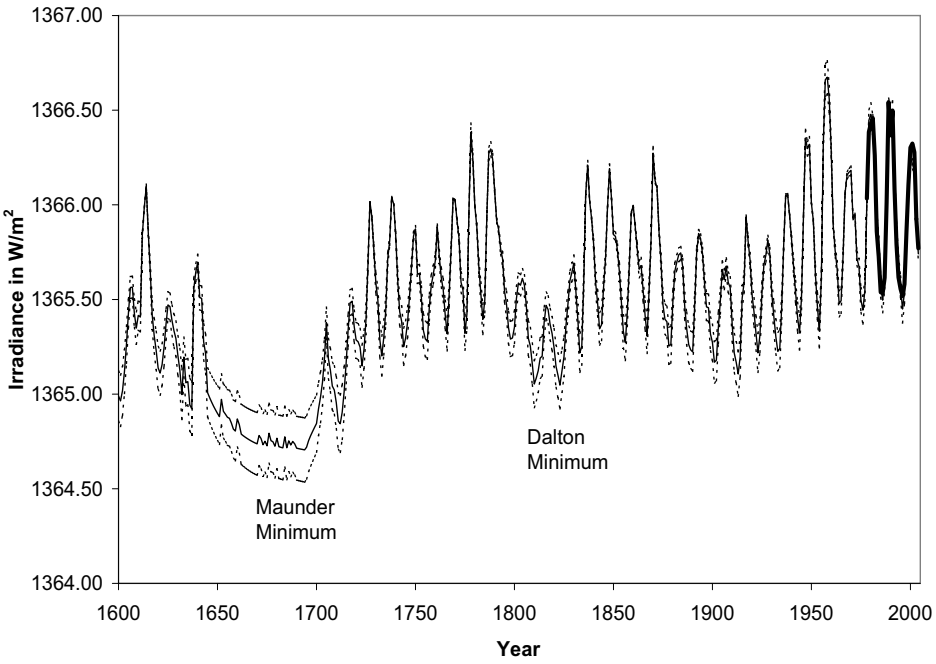

Figure 10. Modelled Irradiance through the Maunder Minimum to the Present. The dotted lines show estimates of the 95% error range, as discussed in the next section. The data plotted with thick lines are the observed irradiance data. The Maunder and Dalton Mimima are marked.

The resulting estimated record of historical irradiance since the Maunder Minimum is shown in Figure 10. The values before the onset of the Maunder Minimum are questionable in that the sunspot number data come from a more indirect source, and the model was still initializing. According to this calculation, the smoothed irradiance (with the cyclic modulation due to the solar activity cycle removed) record shows the irradiance during the Maunder Minimum to be about 1.25 Wm^{-2} lower than is the case at present, and that irradiance has been increasing fairly steadily by between 1 and 1.5 Wm^{-2} since the Maunder Minimum ended.

6. Accuracy and Sensitivity to Errors

The process of using sunspot number to estimate irradiance comprises a number of steps, including several empirical fits. A comprehensive Monte Carlo modelling process, taking into account the approximations, estimates of error distributions and the problem of sometimes including errors twice, indicates that the inherently more tedious Monte Carlo process is probably no more reliable than the simple method used below.

The modelled irradiance I_{mod} is an estimate of the observed irradiance I_{obs}, *i.e.* $I_{obs} = E(I_{mod})$. In order to eliminate the need for an intercept as well as a slope, and to avoid dealing with very small changes in relatively large quantities, we define the slope parameter:

$$m = \frac{I_{obs} - \bar{I}_{obs}}{I_{mod} - \bar{I}_{mod}} \tag{19}$$

where I_{obs} and I_{mod} are respectively the observed and modelled irradiances, and $\bar{I}_{obs}$ and $\bar{I}_{mod}$ are their respective averages over the period 1978-2004. Through a regression analysis of the 1978-2004 observed and modelled irradiances, we obtain $m = 0.99276$ with 95% points 0.8633289 and 1.122192. Rearranging to give an estimator of the observed irradiance:

$$I_{obs} = \bar{I}_{obs} + m\,(I_{mod} - \bar{I}_{mod}) \tag{20}$$

Using the 95% values of m, we estimate the error band for the modelled irradiances, taking into account the effect of extrapolation. The resulting estimates of historical irradiance since 1600 are shown in Figure 10.

7. Discussion and Conclusions

The modelling of historical irradiance necessarily involves extrapolation and the use of proxies. A purely physical or analytical approach is currently not possible, and may never be; the issue is too complex. What can be hoped for is convergence in the results of as diverse a set of modelling approaches as possible. While sharing with other studies an undesirably large dependence upon extrapolation and proxies, it is not based upon estimates of facular areas and sunspot blocking. One other objective was, as far as possible, to base the model upon one index only, sunspot number, which forms a uniquely continuous and homogenous record of solar activity over more than 300 years. The model here is based upon the assumption that sunspot blocking and other factors are simply related - on the basis of annual averages - to the total magnetic flux in strong-field elements, and that there is no need to categorize exactly what features are in the strong or weak-field element

categories. On the average the weak field comes from the decay of strong fields, and some of weak field magnetic flux becomes part of the disc field. To include the Maunder Minimum in the calculation requires information on solar activity prior to that time, we use estimates of sunspot activity before the Maunder Minimum provided by Thomson.

Using the sunspot number as the basis index of the model invokes a problem that when comparing it with other indices, there is significant non-linearity at low activity levels. Fortunately, other quantities such as the total active region magnetic flux correlates strongly and linearly with the 10.7 cm solar radio flux ($F_{10.7}$), and even though the relationship between sunspot number and $F_{10.7}$ is not linear, the correlation is so high that sunspot number, via an empirical relationship can be used to estimate $F_{10.7}$, and thence the total strong-field magnetic flux, which is the required input quantity for the model.

The conclusion indicated here is that during the Maunder Minimum, the solar total irradiance was between 1 and 1.5 Wm^{-2} lower than it is at present. This is a little over half the value obtained by Lean (2000). That no explicit invocation of sub-photospheric modulation of radial energy flow or solar radius changes were made in the model may be assumed to support the assertation by for example Foukal and Lean (1988) that irradiance variations can be fully explained in terms of the differing emissivities of the various classes of photospheric structure, in particular sunspots, faculae and elements of the active network. However, a note of caution is required. In this model a significant contribution in the variability comes from the so called "disc field" elements, which are estimated in a rather tenuous manner from the weak-field flux. There is a possibility that the weak-field contribution is something else, perhaps a variation in solar radius with activity level, with the concomitant variations in background disc emissivity. See for example the discussion by Foukal and Spruit (2004). Since all the visible manifestations of solar activity are strongly modulated by the magnetic activity cycle, it is difficult in many cases to identify reliably what phenomena are causally rather than coincidentally related. In the case here, we do not conclude that this model may rule out sub-photospheric modulation, and there is accordingly a need for more research into the balance between photospheric and subphotospheric modulation of the Sun's energy output.

Acknowledgements

Firstly we would like to thank Karen Harvey for providing the magnetic flux budget data for a range of thresholds over a solar activity cycle. These were derived from magnetograms from the National Solar Observatory at Kitt Peak, which is operated cooperatively by the National Science Founda-

tion/National Optical Astronomy Observatories, National Aeronautics and Space Administration/Goddard Space Flight Center, and National Oceanic and Atmospheric Administration/Space Environment Laboratory. We also thank David Thomson of Queen's University, Kingston, Ontario, for constructing a composite record of sunspot number prior to the Maunder Minimum. Hélène Paquette thanks the National Research Council Summer Student Programme for supporting her participation in this project. The database of measurements of total irradiance was obtained from Physikalisch-Meteorologisches Observatoriu Davos, and a very special thanks is due to those who laboured to produce, from a number of different databases, a continuous record of observed irradiance covering almost three solar activity cycles. The sunspot data from 1700 onwards were downloaded from the National Geophysical Data Center at Boulder, Colorado, magnetic flux data were obtained from the National Solar Observatory at Kitt Peak, and the 10.7 cm solar radio flux data are provided as a service by the National Research Council of Canada.

References

Anderson R.Y.: 1991. 'Solar variability captured in climatic and high-resolution palaeoclimatic records: a geologic perspective'. In: Sonett C.P., Giampapa M.S., Matthews M.S. (Eds), *The Sun in time*, University of Arizona Press, 543-561.

Antia H.M.: 2003. 'Does the Sun Shrink with Increasing Magnetic Activity?'. *Astrophys. J.*, **590**, 567.

Bhatnagar A., Jain K., Tripathy S.C.: 1999. 'Gong p-mode frequency changes with solar activity.' *Astrophys. J.*, **521**, 885-888.

Delache Ph, Lacrare F., Sadsaout H.: 1986. 'Long periods in diameter, irradiance and activity of the Sun'. In: Christensen-Dalsgaard J., Frandsen S. (Eds), *Advances in Asterioseismology*, IAU Press, 223-226.

Eddy J.A.: 1976 (a). 'The Maunder Minimum'. *Science*, **192**, 1189-1202.

Eddy J.A.: 1976 (b). 'The Sun since the Bronze Age', In: Willaims D.G. (Ed.), *Physics of solar planetary environments*, American Geophysical Union, Washington, DC, 958-972.

Eddy J.A.: 1977. 'Historical evidence for the existence of the solar cycle'. In: White O.R. (Ed.) *The solar output and its variation*, University of Colorado Associated University Press - Boulder, 51-71.

Eddy J.A.: 1979. 'The new Sun: the solar results form skylab', *NASA - SP402*.

Eddy J.A.: 1980. 'The historical record of solar activity'. In: Pepin R.O., Eddy J.A., Merril R.B. (Eds), *The ancient Sun: fossil record in the Sun, Moon and meteorites*, Pergamon Press, New York, 119-134.

Foukal P., Lean J.: 1988. 'Magnetic modulation of solar luminosity by photospheric activity', *Astrophys. J.*, **328**, 347-357.

Foukal P., Spruit H.: 2004. 'Comment on "Variations of Total Irradiance Produced by Structural Changes in the Solar Interior " '. *EOS*, **49**, 524.

Fox P., Sofia S. 1994. 'Convection and Irradiance Variations'. In: Pap J.M., Hudson H.S., Solanki S.K. (Eds), *The Sun as a Variable Star: Solar and Stellar Irradiance Variations*, Cambridge University Press, 280-290.

Fox P.: 2004 'Solar Activity and Irradiance Variations'. In. In: Pap J.M., Fox P. (Eds), *Solar Variability and its Effects on Climate*, Geophysical Monograph Series No. 141, American Geophysical Union, 141-170.

Fröhlich C., Foukal P.V., Hickey J.R., Hudson H.S., Willson R.C.: 1991. 'Solar irradiance variability from modern measurements'. In: Sonett C.P., Giampapa M.S., Matthews M.S. (Eds), *The Sun in time*, University of Arizona Press, 11-29.

Fröhlich C.: 1994. 'Irradiance Variations in the Sun'. In: Pap J.M., Hudson H.S., Solanki S.K. (Eds), *The Sun as a Variable Star: Solar and Stellar Irradiance Variations*, Cambridge University Press, 28-36.

Fröhlich C., Lean J.: 1998. 'Total Solar Irradiance Variations.', in *New Eyes to see inside the Sun and Stars*, F.L.Deubner et al., Eds., Proceedings IAU Symposium 185, Kyoto, August 1997, Kluwer Academic Publ., Dordrecht, The Netherlands, pp. 89-102.

Fröhlich C., Lean J.: 1998. 'The Sun's total irradiance: cycles, trends and related climate change uncertainties since 1978.', *Geophys.Res.Let.*, **25**, 4377-4380.

Fröhlich C.: 2004. 'Solar Irradiance Variability'. In: Pap J.M., Fox P. (Eds), *Solar Variability and its Effects on Climate*, Geophysical Monograph Series No. 141, American Geophysical Union, 97-110.

Gaizauskas V., Harvey K.L., Harvey J.W., Zwaan C.: 1983. 'Large-scale patterns formed by active regions during the ascending phase of Cycle 21'. *Astrophys, J.*, **265**, 1056-1065.

Gray D., Livingston W.: 1997.'Monitoring the solar temperatureL spectroscopic temperature variations of the Sun.' *Astrophys. J.*, **474**, 802-809.

Harvey K.L.: 1992. 'Measurement of Solar Magnetic Fields as an Indicator of Solar Activity Evolution.' In: Donnelly R.F. (Ed.), *Proceedings of the Workshop on the Solar Electromagnetic Radiation Study for Solar Cycle 22*, NOAA/ERL/SEL, Boulder, Colorado, 113-129.

Harvey K.L.: 1994. 'Irradiance models based upon solar magnetic fields.' In: Pap J.M., Hudson H.S., Solanki S.K. (Eds), *The Sun as a Variable Star: Solar and Stellar Irradiance Variations*, Cambridge University Press, 217-225.

Hoyt D.V., Schatten K.H.: 1995*a*, 'Overlooked sunspot observations by Helvelius in the early Maunder Minimum, 1653-1684', *Solar Physics*, **160**, 371-378.

Hoyt D.V., Schatten K.H.: 1995*b*, 'Observations of sunspots by Flamsteed during the Maunder Minimum', *Solar Physics*, **160**, 379-385.

Hoyt D.V., Schatten K.H.: 1996, 'How well was the Maunder Minimum observed?', *Solar Physics*, **165**, 181-192.

Hoyt D.V., Schatten K.H.: 1998*a*, 'Group sunspot numbers: a new solar activity reconstruction', *Solar Physics*, **179**, 189-219.

Hoyt D.V., Schatten K.H.: 1998*b*, 'Group sunspot numbers: a new solar activity reconstruction', *Solar Physics*, **181**, 491-512.

Krüger A.: 1979. 'Introduction to Solar Radio Astronomy and Radio Physics.' Dordrecht Reidel Publishing Company, Dordrecht, Holland.

Kuhn J.: 1996. 'Global Changes in the Sun'. In: Roca-Cortés T. (Ed.), *The Structure of the Sun: VI Winter School at the Instituto d'Astrophysica de Canarias*, Cambridge University Press, 231-278.

Kuhn J.: 2004. 'Irradiance and Solar Cycle Variability: Clues in Phase Properties.' *Advances in Space Research*, **34**, 302-307.

Kundu M.R.: 1965. 'Solar Radio Astronomy', John Wiley, Publishers.

Lean J.L., Cook J., Marquette W., Johanneson A.: 1998. 'Magnetic sources of the solar irradiance cycle.' *Astrophys. J.*, **492**, 390-401.

Lean J.: 2000. 'Evolution of the Sun's spectral irradiance since the Maunder Minimum.' *Geophysical Research Letters*, **27**, No. 16, 2425-2428.

Pap J.M., Fröhlich C.: 1999. 'Total solar irradiance variations.' *Journal of Atmospheric and Solar-Terrestrial Physics*, **61**, 15-24.

Parker E.N.: 1994. 'Theoretical interpretation of magnetic activity'. In: Pap J.M., Hudson H.S., Solanki S.K. (Eds), *The Sun as a Variable Star: Solar and Stellar Irradiance Variations*, Cambridge University Press, 264-269.

Ribes E., Mein P., Mangeney A.: 1985. 'A large-scale meridional circulation in the convective zone'. *Nature*, **318**, 170-171.

Sofia S.: 2004. 'Variations of Total Solar Irradiance Produced by Structural Changes in the Solar Interior'. *EOS. Trans. AGU.*, **22**, 217.

Sofia S., Li L.: 2004. 'Solar Variability Caused by Structural Changes in the Convection Zone.' In *Solar Variability and its Effects on Climate. Geophys. Monogr. Ser.***141**

Solanki S.K., Unruh Y.C.: 1998. 'A model for the wavelength dependence of solar irradiance variations. ' *Astron. Astrophys.* **329**, 747-753.

Solanki S.K., Schüssler M., Fligge M.: 2000, 'Evolution of the Sun's large-scale magnetic field since the Maunder Minimum.', *Nature*, **408**, 445-447.

Solanki S.K., Schüssler M., Fligge M.: 2002, 'Secular variation of the Sun's magnetic flux.', *Astron. Astrophys.*, **383**, 706-712.

Spruit H.: 2000. 'Theory of Solar Irradiance Variations', *Space Sceicne Reviews*, **94**, 113-126.

Tapping K.F.: 1987. 'Recent solar radio astronomy at centimeter wavelengths: the temporal variability of the 10.7-cm flux.' *J. Geophys. Res.*, **92**, No. D1, 829-838.

Tapping K.F., Harvey K.L.: 1994. 'Slowly-varying microwave emissions from the solar corona'. In: Pap J.M., Hudson H.S., Solanki S.K. (Eds), *The Sun as a Variable Star: Solar and Stellar Irradiance Variations*, Cambridge University Press, 182-195.

Tapping K.F., Zwann C.: 2002. 'Sources of the slowly-varying component of solar microwave emission and their relationship with their host active regions.' *Solar Physics*, **199**, 317-344.

Tapping K.F., Cameron H.T., Willis A.G.: 2003. 'S-component sources at 21 cm wavelength in the rising phase of Cycle 23.', *Solar Physics*, **215**, 357-383.

Ulrich R., Bertello L.: 1995. 'Solar cycle dependence of the Sun's photospheric radius in the neutral iron spectral line of 525.5 nm', *Nature*, **377**, 214-215.

Willson R.C., Hudson H.S.: 1991. 'The Sun's luminosity over a complete solar cycle.', *Nature*, **351**, 42-44.

Woodard M.F.: 1987. 'Frequencies of low-degree solar acoustic oscillations and the phase of the solar cycle', *Solar Physics*, **114**, 114-128.

Zwaan C., Harvey K.L.: 1994. 'Patterns in the Solar Magnetic Field', In: Schüssler M., Schmidt W. (Eds), *Solar Magnetic Fields*, Cambridge University Press, 27-48.